LA-UR- 11-03728

Approved for public release; distribution is unlimited.

Title:	The Role of the Structure of Grain Boundary Interfaces During Shock Loading
Author(s):	Alejandro G. Perez-Bergquist, Juan P. Escobedo, Carl P. Trujillo, Ellen K. Cerreta, George T. Gray III, Christian Brandl, and Timothy C. Germann
Intended for:	American Physical Society - Shock Compression of Condensed Matter Conference

Los Alamos National Laboratory, an affirmative action/equal opportunity employer, is operated by the Los Alamos National Security, LLC for the National Nuclear Security Administration of the U.S. Department of Energy under contract DE-AC52-06NA25396. By acceptance of this article, the publisher recognizes that the U.S. Government retains a nonexclusive, royalty-free license to publish or reproduce the published form of this contribution, or to allow others to do so, for U.S. Government purposes. Los Alamos National Laboratory requests that the publisher identify this article as work performed under the auspices of the U.S. Department of Energy. Los Alamos National Laboratory strongly supports academic freedom and a researcher's right to publish; as an institution, however, the Laboratory does not endorse the viewpoint of a publication or guarantee its technical correctness.

Form 836 (7/06)

THE ROLE OF THE STRUCTURE OF GRAIN BOUNDARY INTERFACES DURING SHOCK LOADING

A. G. Perez-Bergquist[1], J. P. Escobedo[1], C. P. Trujillo[1], E. K. Cerreta[1], G. T. Gray III[1], C. Brandl[2], and T. C. Germann[2]

[1]*Materials Science and Technology Division, Los Alamos National Laboratory, Los Alamos, NM 87545, USA*
[2]*Theoretical Division, Los Alamos National Laboratory, Los Alamos, NM 87545, USA*

Abstract. In order to understand the role of interface structure during shock loading, and specifically the role of interfaces in damage evolution due to shock, four copper bi-crystal grain boundaries (GBs) were studied under shock loading and incipient spall conditions. These boundaries, two [001]/[111] boundaries and two [001]/[001] boundaries, were characterized prior to deformation using optical microscopy (OM), electron back scattered diffraction (EBSD), and transmission electron microscopy (TEM) to determine axis/angle pair relationships and interface plane. Samples containing these boundaries were then subjected to incipient spall at 2.5 GPa and shock loading at 10 GPa, respectively, in an 80 mm gas gun. Samples were soft recovered and characterized post-mortem via EBSD and TEM. Preliminary results indicate that typical GBs readily form damage during shock loading but that special boundaries, such as twin boundaries, are resistant to failure. Differences in slip and defect transmissibility across these types of boundaries likely play a role in the failure modes.

Keywords: Grain boundaries, Copper, TEM.
PACS: 62.20.M, 81.40.Vw, 81.70.Bt.

INTRODUCTION

Over the past several decades, numerous studies have shown that dynamic damage evolution in structural materials is strongly dependent upon interface interactions [1-3], but often, investigation of dynamic damage evolution at interfaces has involved techniques with resolution length scales that are too large to characterize unit processes associated with the role of interface structure. As a result, few studies have interrogated the role of atomic-scale interface structure on dynamic damage evolution. Here, we investigate the role of interfaces in damage evolution due to shock by systematically examining the interface structure of bi-crystalline samples with varying orientation relationships and interface structures. We find that GB structure plays a much greater role than grain orientation in damage evolution.

EXPERIMENTAL PROCEDURES

A high purity Cu multi-crystal was grown at Los Alamos National Laboratory using a Bridgman furnace to control the crystallographic orientations of the Cu grains. The multi-crystal was then sectioned into disks 25.4 mm in diameter and 5.1 mm in thickness. A sample disk is shown in Fig. 1, with grain orientations and GB types identified.

Two separate shock recovery experiments were performed using an 80 mm single stage gas gun, a conventional shock compression experiment as well as a damage experiment where pressure release waves were allowed to interact within the

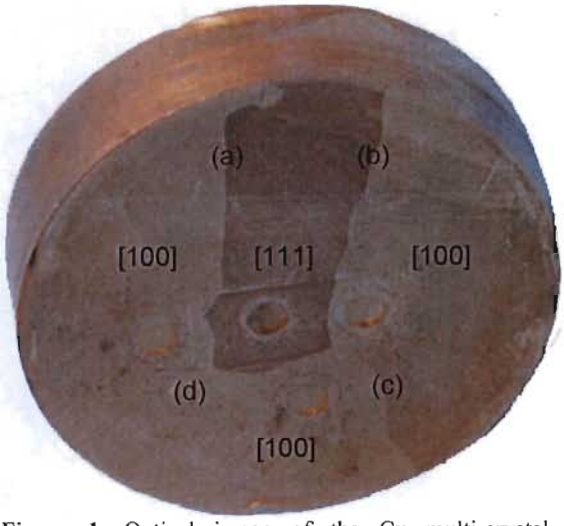

Figure 1. Optical image of the Cu multi-crystal. Crystallographic surface normal orientations for each grain are shown. The grain boundaries consist of a) an [001]/[111] twin boundary (60°), b) an [001]/[111] high angle boundary (~50°), c) an [001]/[001] tilt boundary (28°), and d) an [001]/[001] low angle boundary (~2°).

multi-crystal. For the shock experiment, the Cu multi-crystal was tightly fitted into inner and outer momentum trapping rings and was protected from impact and spallation by a close fitting cover plate and spall plates, respectively. In the damage experiment, the sample was also fitted into inner and outer momentum trapping rings, but the sample was not protected from spallation by a spall plate. For both experiments, shock direction was perpendicular to the disk face and nearly in the plane of each GB. All sample assembly components were fabricated from copper to ensure impedance matching during shock loading.

In the shock experiment, the Cu multicrystal was shocked to a peak shock pressure of 10 GPa, while in the damage experiment, the sample was impacted to a peak shock pressure of only 2.1 GPa so as to not cause complete spallation of the Cu multi-crystal. Peak shock pressures were calculated from free surface velocities taken by photonic doppler velocimetry (PDV). Following impact, samples were soft recovered and reserved for post-mortem analysis.

Samples were observed via OM, EBSD, and TEM. OM was performed using a Zeiss optical microscope equipped with an Axiocam HRc digital camera, and EBSD was performed using a Philips XL30 SEM equipped with a Hikari high speed EBSD detector. Data was acquired and analyzed using orientation imaging microscopy (OIM) software by TexSEM Laboratories (TSL) of EDAX. TEM foils were prepared either by electrolytic thinning or by *in situ* fabrication and liftout in a Helios NanoLab DualBeam combination scanning electron microscope (SEM) and focused ion beam (FIB) system. TEM observations were performed using an FEI Tecnai F30 analytical TEM operating at 300kV. In this paper, TEM data presented is from the 10 GPa shock experiment while EBSD data presented is from the 2.1 GPa damage experiment.

RESULTS AND DISCUSSION

OM of the electrochemically prepared TEM foils showed little difference between the undeformed and deformed samples at the [001]/[111] high angle GB, but images taken of the undeformed and deformed [001]/[111] Σ3 twin GB revealed a significant difference in the GB morphology before and after shock. While the GB appeared almost linear in the undeformed specimen, the shocked specimen contained large scale jogs across the length of the boundary, as shown in Figure 2. The results of the OM necessitated further investigation of the boundary via TEM.

TEM performed on bulk regions (>100 μm from the nearest GB) of the shocked [100] and [111] grains showed that substructure evolution is dependent upon grain orientation. [100] grains exhibited loose dislocation tangles but not well developed dislocation cells. [100] grains also showed extensive deformation twinning. Localized regions exhibited primarily one deformation mechanism, however, as heavily twinned areas had a qualitatively lower dislocation density than twin free regions. The [111] grain did not exhibit deformation twinning, but did possess more extensive dislocation formation and better-defined dislocation cells. The influence of crystallographic orientation on stress state and its effect on twinning has been discussed in a previous work [4].

TEM of the undeformed and shocked grain boundaries revealed unique behavior of certain boundaries in response to shock. Despite small

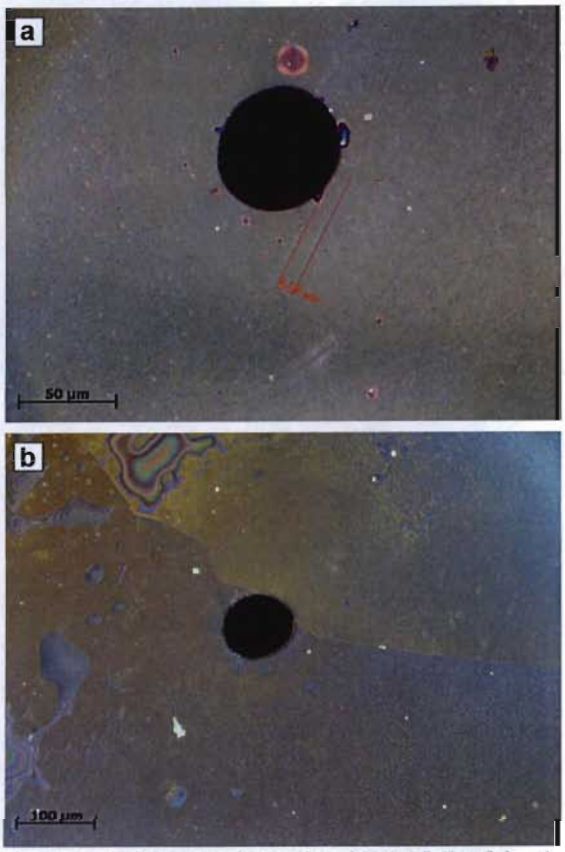

Figure 2. OM images of jetpolished TEM foils of the a) undeformed and b) deformed [001]/[111] Σ3 twin GB.

local defects, both the [001]/[111] Σ3 twin GB and the [001]/[111] high angle GB appeared relatively planar in the undeformed samples. After shock, the high angle GB retained its initial structure, but the Σ3 twin GB developed large-scale, periodic steps along the entire length of the boundary. The steps were visible across the entire width of the FIB-fabricated TEM foil, occurring on average about every 200 nm, though steps were seen to occur anywhere from 50 to 350 nm apart along the GB. The length of the steps as projected on the TEM image averaged 50 nm, but some steps projected as large as 85 nm in width. Since the actual steps are undoubtedly three-dimensional in nature, the actual lengths of the steps are actually larger than that reported. Combined, these small steps compose the macroscopic jogs seen in Figure 2.

Crystallographic analysis of the shocked samples shows that the step ledges are aligned with $\{111\}\langle 1\bar{1}0\rangle$ slip systems for F.C.C. copper, whereas the GB sections between steps are not oriented along any particular major crystallographic direction. While the steps could be due to faceting during crystal growth, TEM on the undeformed samples showed no evidence of such formation, leaving two main possible mechanisms for the formation of the steps under shock given their orientations. One possibility is that dislocation generation due to shock led to massive dislocation accumulation at the GB and that these dislocations then transmitted across the boundary along slip planes. While possible, given the sheer magnitude of dislocations needed to create steps of the sizes observed, one would expect to see post-mortem evidence of dislocation pile-up, such as dislocation banding, at the GB, which has not been observed in TEM images thus far. Another possible mechanism for step formation is coupled GB motion. Under this mechanism, GB migration would occur due to emission of Shockley partial dislocations from the boundary, and the dislocation content for motion would already be present in the GB as opposed to being introduced during shock compression. Current molecular dynamics simulations that mimic these experiments suggest that GB motion is due to the latter mechanism, but more analysis, including additional modeling, high resolution TEM of the deformed and undeformed boundary structure, and Schmid factor analysis, are necessary before either mechanism can be fully validated.

EBSD performed on the samples spalled at 2.1 GPa also revealed noticeable differences between the behaviors of the four grain boundaries. Figure 3 shows an optical microscope collage of a cross-sectional slice of the 2.1 GPa shocked sample containing the [001]/[111] Σ3 twin GB and the [001]/[111] high angle GB. Also in the image are EBSD scans from near the spall plane at each boundary. At the Σ3 interface, void nucleation occurred but did not seem to be influenced by the presence of the boundary, or in other words, void nucleation at the interface seems virtually identical to void generation in the bulk of either the [100] or [111] grain. However, void nucleation behaved distinctly different at the high angle GB. At this interface, voids seem to have preferentially formed at the boundary, resulting in the formation of a large void right at the interface. It should be

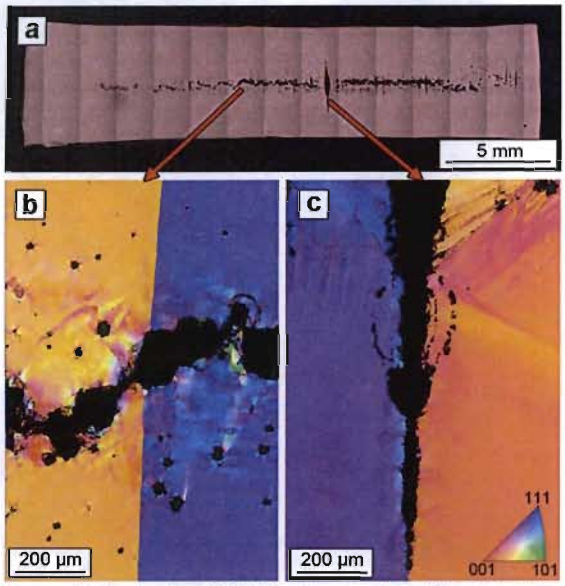

Figure 3. Optical and EBSD micrographs of the 2.1 GPa spalled Cu sample. a) Cross-sectional optical image of the shocked disk. b) EBSD scan of the Σ3 twin boundary. c) EBSD scan of the ~50° high angle boundary. Legend for the EBSD micrographs is shown at bottom right.

emphasized that these two interfaces have the same orientations on either side of the GB, so the difference in damage evolution is not due to crystallographic differences or the sound speed differential at the boundary. Thus, the difference in damage evolution at each interface must necessarily be due to boundary structure and its response to dislocation generation during shock. EBSD analysis of the [100]/[100] tilt and low angle boundaries showed that the 28° tilt GB behaved very similarly to the ~50° high angle GB, while the ~2° low angle GB behaved essentially the same as the Σ3 GB. EBSD analysis from shocked polycrystalline Cu samples also showed that Σ3 interfaces consistently are more resistant to damage nucleation than other generalized grain boundaries.

CONCLUSIONS

The combination of results from the two shock experiments may be evidence of the role of GB structure for damage tolerance. In the 10 GPa pure shock test, the Σ3 interface faceted dramatically, whereas the ~50° high angle GB remained stationary. In the 2.1 GPa spall experiment, the high angle GB experienced severe void nucleation and coalescence, leading to boundary failure, while the Σ3 did not. Combined, these two pieces of data seem to indicate that the Σ3 GB is able to relieve stress through dislocation/boundary structure interactions that facet the shocked boundary. Other more generalized boundaries do not activate this same mechanism, making them more susceptible to damage nucleation. One could envision a scenario where dislocations are able to easily transmit through Σ3 interfaces but not though other boundaries, causing residual stresses that lead to damage formation at those boundaries; however, more work is needed before any mechanisms for Σ3 grain GB motion can be validated. What is clear, however, is that GB structure plays a significant role in the morphology of and damage evolution at GBs.

ACKNOWLEDGEMENTS

Los Alamos National Laboratory is operated by LANS, LLC, for the National Nuclear Security Administration of the US Department of Energy. This work has been performed under the auspices of the US Department of Energy and supported by the Office of Basic Energy Sciences Energy Frontier Research Center for Materials at Irradiation and Mechanical Extremes (CMIME).

REFERENCES

1. Christy, S., Pak, H. R., and Meyers, M. A.: *Metallurgical Applications of Shock-Wave and High Strain-Rate Phenomena*, Murr, L. E., Staudhammer, K. P., and Meyers, M. A., eds., Marcel Dekker, New York, NY, 1986, pp. 835-63.
2. Hong, S. I., Gray III, G. T., and Lewandowski, J. J., *Acta Metall. Mater.* 41, 1993, pp. 2337-2351.
3. Zurek, A. K. and Meyers, M. A.: *High-Pressure Shock Compression of Solids II*, Davison, L., Grady, D. E., and Shahinpoor, M. eds., Springer-Verlag, New York, NY, 1996, pp. 25-70.
4. Cao, F., Beyerlein, I. J., Addessio, F. L., Sencer, B. H., Trujillo, C. P., Cerreta, E. K., and Gray III, G. T., *Acta Mater.* 58, 2010, pp. 549-559.